



**University of
Sunderland**

Naveed, Nida (2020) Investigate the effects of process parameters on material properties and microstructural changes of 3D printed specimens using Fused Deposition Modelling (FDM). *Materials Technology: Advance Performance Materials*, ahead. p. 1. ISSN 1066-7857

Downloaded from: <http://sure.sunderland.ac.uk/id/eprint/11897/>

Usage guidelines

Please refer to the usage guidelines at <http://sure.sunderland.ac.uk/policies.html> or alternatively contact sure@sunderland.ac.uk.

Investigate the effects of process parameters on material properties and microstructural changes of 3D printed specimens using Fused Deposition Modelling (FDM)

N. Naveed

Faculty of Technology, University of Sunderland, Sunderland, SR6 0DD, UK

Email: nida.naveed@sunderland.ac.uk

Abstract

One of the most significant parameters of the Fused Deposition Modelling (FDM) for 3D printing process is the raster angle. In this study, the five different raster angles are used to fabricate the 3D parts using thermoplastic material - polylactic acid (PLA), and tensile properties of these parts are investigated to identify the best raster position to fabricate the strongest 3D printing part. In this study, the microstructural analyses on fracture interface, and on outer and inner surfaces of these 3D parts are performed using a scanning electron microscopy (SEM) to examine material failure modes and reasons, and defects in the 3D parts. This study identified the best raster orientation to lie down the layers of 3D printing material during the process. This study also identified that there are several defects in 3D printed parts at micro level that have large impact on mechanical properties of 3D printed part.

Keywords: 3D printer, PLA, Fused deposition modelling (FDM), additive manufacturing (AM), microstructural analysis, raster angles, scanning electron microscopy (SEM), tensile test.

Introduction

Additive Manufacturing (AM) is a process that can join materials in an additive way (layer upon layer) to make complex physical parts from 3D digital models. This manufacturing technique can be categorised into three fundamental groups such as liquid based, solid based and powder based. Liquid based AM technique construct an object in liquid or high viscose material state and then use heat to harden the object such as material jetting and VAT Photopolymerization [1]. Solid state AM technique use solids in one form or another to create an object such as fused deposit system and Ultrasonic consolidations [2], [3]. Powder based AM technique such as powder bed fusion (PBF) methods use either a laser or electron beam to melt and fuse material powder together [4], [5].

3D printing, is referred to as solid state AM technique, is a process of making an object in three dimensions by stacking up multiple best thin layers of selected material. The first step of this process is to produce a digital model using a CAD software and transfer it into the 3D printer machine to turn it into a physical object [6]. This technology becomes more famous for fast manufacturing process for the small industries and personnel usage. The most significant advantage for 3D printing is that it can speed up the production process compared to the traditional method of manufacturing [7]. Complicated designs can be uploaded from a SolidWorks software in digital forms to the 3D printers and can be printed in a few hours' time [8]. This technology can be applicable in various fields such as medical sciences [9],[10], construction, automotive, aerospace and architecture [11]–[13]. It has great potential in the medical industry. A Kumar et al elucidated the scope of 3D printing technology for tissue engineering such as development of 3D scaffolds for tissue regeneration [14]–[16]. These studies also discussed the biocompatibility and mechanical properties of 3D scaffolds that are fabricated with different 3D additive manufacturing approaches and concluded that the technology is envisaged to meet the requirements of the biomedical industry. However, some of these applications are still under investigation and considerable research is required to improve their product performance. Moreover, one of the biggest advantages of the materials used for the additive manufacturing processes can be recycled and it can be used back [17], [18]. The small products can be printed using 3D printer with small cost compared to traditional manufacturing process. However, the cost of the large parts in 3D printer is high compared to the traditional manufacturing method [19], [20]. The 3D printing technique is on board from the last three decades, but it is still an under developing technology. This technique requires deep research to get more information so that it extends can be understood and the benefits of this technology can be increased.

There are number of raw materials being used in additive manufacturing processes include metals, alloys, plastics, and other substances in the form of liquids, sheets, powders, and filaments for various applications. Titanium alloys have been electron and laser beam printed and studied for biomedical and mechanical response [21], [22]. The thermoplastic filaments are most commonly used in Fused deposition modelling to fabricate the 3D parts. These materials include acrylonitrile butadiene styrene

(ABS), polycarbonate (PC), polylactide (PLA) and Polyamide (PA)[23], [24]. PLA is the one of the most popular materials in 3D printing due to its low cost, good stiffness and strength, high reliability and good dimensional accuracy and surface finish [25], [26]. PLA is a polymer, called polylactic acid which made from the organic and renewable resource such as potato starch and sugar cane. It is easy to print with, compared to other 3D printer material such as ABS. It is strong but more brittle compared to ABS [27]. It has low coefficient of thermal expansion which limits its applications where the printed part is exposed to temperature higher than 50 °C [28], [29].

Fused deposition modelling (FDM) is one of the popular AM techniques for fabricating plastic parts due to its low cost, minimal wastage and ease of material change [20]. However, FDM is a complex process which is based on many parameters [30], [31]. These parameters can be categorised into four groups such as, part depositing parameters, FDM machine settings, filament properties and environmental factors. Part depositing parameters are infill speed, infill pattern, layer thickness, raster angles, raster width, air gap and contour width. FDM machine settings include nozzle temperature, nozzle diameter, print bed temperature. Filament material properties include its density and colour. Environmental factors include temperature and humidity [32]. Any small change of these process parameters can influence the part quality and material properties. There are limited investigations have been reported on the effect of FDM process parameters on material properties. Therefore, it is crucial to investigate FDM process parameters to ensure the good quality of the parts using this technique. Different studies investigated different 3D printing process parameters and identified their influence on material properties and its behaviour. The raster width and air gaps had been identified as important parameters in affecting the material porosity and mechanical strength [33]. The one of the previous studies pointed out the five important process parameters (layer thickness, orientation, raster angle, raster width and air gap) that have large influence tensile, flexure and impact strength of 3D printed part made up with ABS material [34]. In another study, the two raster orientations, one is cross (0°/90°) and other one is crisscross (45°/-45°) direction were investigated using ABS material and found crisscross (45°/-45°) orientations provides better material strength compared to the other orientation [35]. In another previous study, the effect of layer height, infill density, layer orientation on the mechanical properties of PLA and ABS were investigated and identified that PLA is more suitable for the use of 3D printing material [36]. Letcher et al [37] investigated the three raster orientations 0°, 45° and 90° using PLA material and identified that the 45° raster orientation provided a strongest material behaviour. However, it was not identified that the material behaviour when the raster angle is gradually increased from 0° to 90°. What are microstructural changes occurred within the 3D parted part while using different raster angles. Raster orientation is one of the most important parameters of FDM 3D printing process. Raster orientation – part build orientation refers to the inclination of a part in a build platform with respect to X, Y and Z axis as shown in Figure 1. The X and Y axes represent the plane parallel to build platform and Z axis represents the vertical plane along the direction of the part build [34]. In this study, part depositing parameter – raster orientation is studied and five different raster orientation angles (0°, 30°, 45°, 60° and 90°) are investigated, and three specimens with each raster angle orientation setting are printed. The tensile test is performed for each 3D printed specimen and the effects of this process parameter is investigated on its tensile strength. The micro structural analysis on fracture interface of the specimens after tensile testing are also performed using the scanning electron microscope to explain material failure modes and reasons. In this study, the micro-level structural changes on outer and inner surfaces of the 3D parts that are fabricated using the five different raster orientations are also examined in detail.

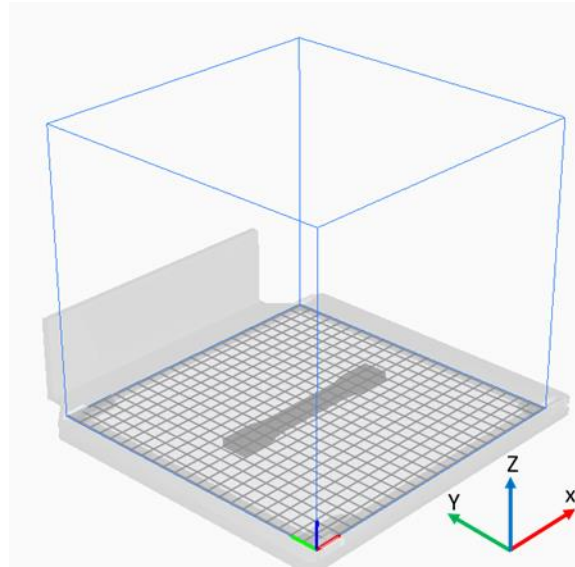


Figure 1: Tensile specimen on 3D printer bed – Image is captured from 3D printer software Cura 4.3.0.

3D printing Material Specification

For this study, the standard PLA material is used for 3D printing. Table 1 and Table 2 show the specifications and mechanical properties of PLA filament [38].

Table 1: PLA Filament specifications

Diameter	2.85 ± 0.10 mm
Max roundness deviation	0.10 mm
Net filament weight	750 g
Filament length	95 m

Table 2: Mechanical properties of PLA filament

Tensile modulus	2.34 GPa
Tensile stress at break	45.6 MPa
Elongation at break	5.2 %

Experimental procedures

For this study, the experimental work consists of preparation of standardised tensile test specimens using 3D printer, testing of 3D printed specimens and detailed microstructural analysis of outer and inner surfaces of 3D printed specimens. The information about each step is provided below in detail.

a. The 3D printing process

Firstly, the test specimens were prepared using 3D printer according to the required specifications. For that, the 3D CAD SolidWorks 2019 software was used to develop three-dimensional virtual geometry of the test specimen. The geometry of the specimen was developed according to the ASTM D638 standard tensile test specimen [39] as shown in Figure 2. After developing the virtual specimen geometry, the SolidWorks file was converted into STL format. The 3D printer can accept this format to physically print the specimen. Then, the STL file was transferred to the 3D printer-controlled computer. The 3D printer Ultimaker 5 as shown in Figure 3 was employed to print the specimens as it is a powerful, simple and reliable 3D printer technology. It operates through a touchscreen interface guides and displays detailed status information. The PLA spool is used to print the specimens as shown in Figure 4. Cura 4.3.0 – 3D printing software was used to prepare the design that was developed in SolidWorks for 3D printing. This software can manage, monitor the print progress, maintenance schedules, queue

prints and manage the different software design. For the printing, custom printing settings were used to get in-depth control to the printing software which allow printer to specific printing parameter settings such as different raster orientations. This 3D printer extruded the material at 200 °C at a speed of 70 mm/s with the heated bed surface at 60 °C, this is to prevent warping on the first layer of specimen. The specimens were printed with five different raster orientation angles (0°, 30°, 45°, 60° and 90°) one by one as shown in Figure 5 . The 100% infill density was used for each raster orientations. There were three identical tensile specimens printed with each raster orientation and altogether 18 specimens were printed. All these specimens were built with 1Kg spool of PLA material. This printer starts a printing with the build of a thin layer of base support as shown in Figure 6 and then it builds an outer layer base and fill the specimen with specific raster orientation. The process of the 3D printing for these tensile specimens is shown in Figure 7.

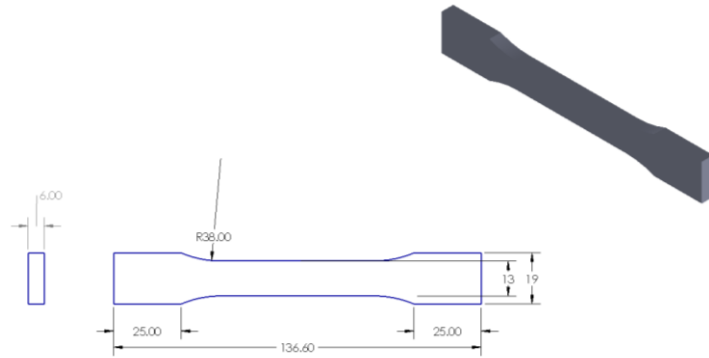


Figure 2: Geometry of the tensile test specimen according to ASTM D638 standard (all dimensions are in mm).



Figure 3: The 3D printer Ultimaker S5



Figure 4: PLA spool – Material used for 3D printing

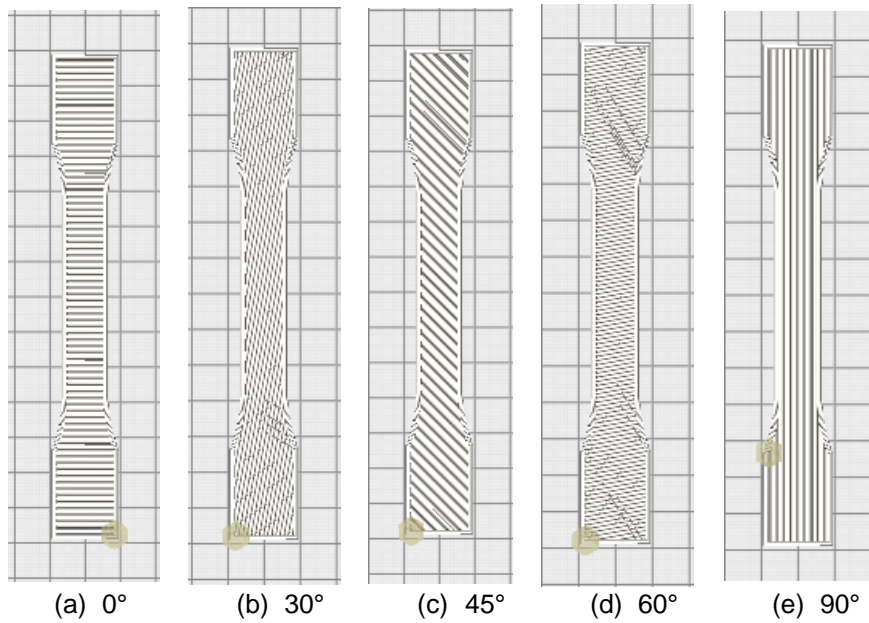


Figure 5: Five raster orientations used – Images are captured from 3D printer software Cura 4.3.0.

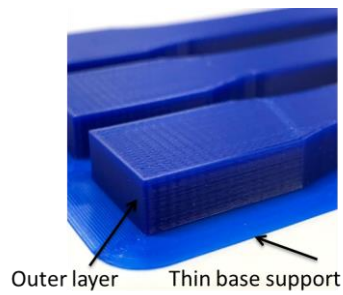


Figure 6: 3D printed specimen

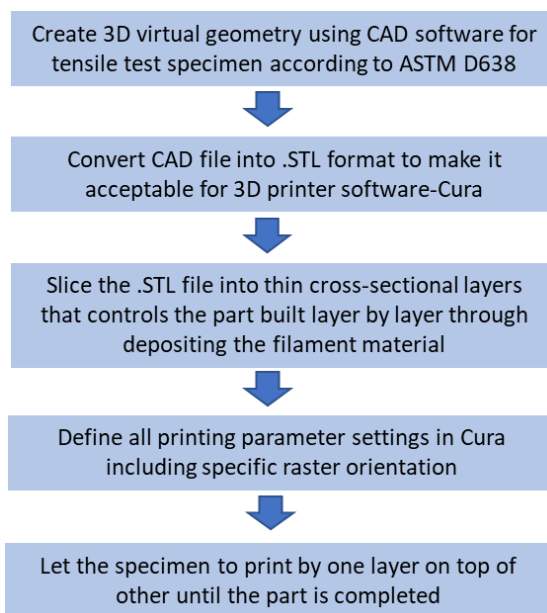


Figure 7: Flow diagram for the process of 3D printing.

b. Tensile testing for 3D printed specimens

All 3D printed specimens were testing according to ASTM D638 standard testing method for tensile testing of plastics material [39]. Universal tensile testing machine was used to conduct the tensile test. The specimens were tested at a speed of 5 mm/min. Specimens were set for this test machine using the desktop testXpert2 software. This software also collected the displacement (mm) and force (N) values for each test in order to obtain stress-strain curves. Figure 8 shows the tensile test set up to perform the test for 3D printed specimens.

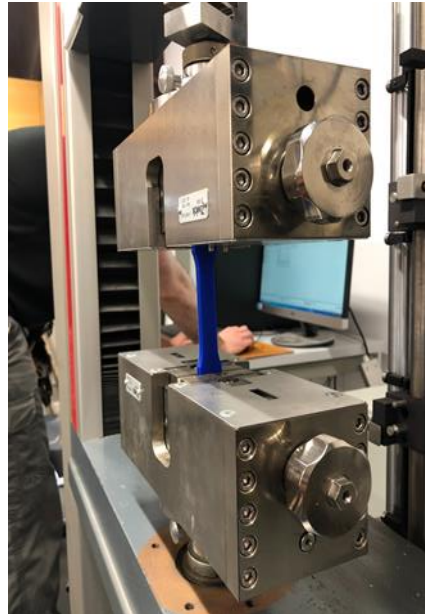


Figure 8: shows the tensile test set up to perform the test for 3D printed specimens.

c. Sample preparation for microstructural examination

Material strength of any material directly relates to its microstructure. Therefore, the microstructure examination of the fractured surface is vital to understand the failure behaviour and failure mode. In this study, the fractured interface of the tensile specimens after the tensile testing were analysed. In addition to this, the outer surfaces of the tensile specimens are also examined to identify any defect formed during 3D printing. In this study, Scanning Electron Microscope (SEM) S-3000N, Hitachi was used at an acceleration of 5 KV with high vacuumed mode to examine microstructure of the material. In order to prepare the samples for SEM analysis, specimens were broken into small pieces along the fractured surfaces. Then, the samples were vacuum sputter coated with a thin layer of gold-palladium alloy to eliminate the charging effects of the surface. This thin layer coating is important as it provides a homogeneous surface for analysis and imaging.

Results and discussions

a. Tensile test

There are three identical tensile specimens were tested with each raster orientation. The individual results for each test are shown in Table 3 and the summary of all the tensile test results are given in Table 4.

Table 3: Tensile test results of 3D printed specimens.

<i>Raster Orientation (degree)</i>	<i>Actual Width (mm)</i>	<i>Actual Thickness (mm)</i>	<i>Elongation at Break (%)</i>	<i>Modulus Elasticity (GPa)</i>	<i>Ultimate Stress (MPa)</i>
0° (1)	13.34	6.02	1.35	1.13	13.71
0° (2)	13.39	5.98	2.081	0.85	15.15
0° (3)	13.39	5.98	2.22	0.85	13.22
30° (1)	13.37	6.01	3.07	0.77	21.06
30° (2)	13.43	6.03	1.89	0.92	14.48
30° (3)	13.36	6.04	2.21	0.85	15.79
45° (1)	13.00	5.87	4.44	1.21	53.94
45° (2)	12.94	5.85	3.93	1.49	54
45° (3)	12.97	5.89	4.34	1.67	58.4
60° (1)	13.35	6.03	1.82	0.79	13.7
60° (2)	13.29	6.05	2.18	0.95	16.8
60° (3)	13.39	6.02	2.03	0.88	15.3
90° (1)	13.35	5.98	3.63	1.73	47
90° (2)	13.39	6.06	3.25	1.81	42.5
90° (3)	13.33	5.98	2.51	1.47	31.5

Table 4: The summary of all the tensile test results

<i>Raster Orientation (degree)</i>	<i>Elongation at Break (%)</i>	<i>Modulus Elasticity (GPa)</i>	<i>Ultimate Stress (MPa)</i>
0°	1.88	0.94	14.03
30°	2.39	0.85	17.11
45°	4.24	1.46	55.45
60°	2.01	0.87	15.27
90°	3.13	1.67	40.33

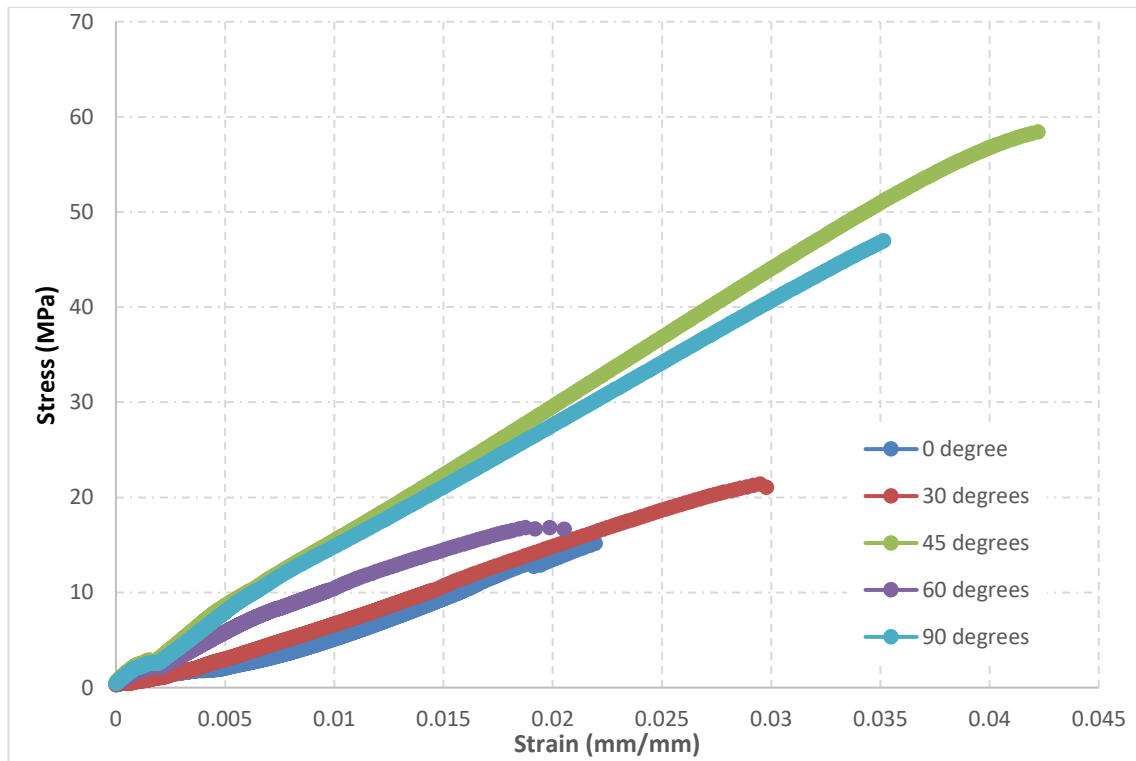


Figure 9: Tensile test results (stress-strain curves) for each of the raster orientation.

Table 3 and Table 4 results show the effect of raster orientation on tensile properties including the ultimate strength, the modulus of elasticity and elongation at break that for the material of PLA. The 45° raster orientation produced a strongest specimen with the average ultimate tensile is 55.45 MPa and highest elongation of 4.24 %. The 90° raster orientations produced the specimen with the average ultimate tensile strength is 40.33 MPa (27% less than the strength of the specimen produced with 45° raster orientation), which is the second highest strength compared to the results of all other printed specimens. The 0°, 30° and 60° orientations produced weak specimens with the average ultimate strength are 14.04 MPa, 17.11 MPa and 15.27 MPa respectively. These results show that the position of raster is an important parameter for 3D printing, and it has a vital role in the specimen strength. Figure 9 shows the stress strain curves for the specimens printed with five different raster orientations. From these curves it can be identified that which specimen have strongest, toughest and brittle material behaviour. In order to identify which orientation produced a strongest specimen, the stress value at break are compared for all these five specimens. The orientation 45° shown a strongest specimen with the value of 55.45 MPa and specimen printed with the orientation of 0° produced a weakest specimen with the value of 14.03 MPa. The specimen printed with the orientations of 45°, 90° and 60° shown both elastic and plastic deformation, therefore these specimens are identified as hard materials. The specimen printed with the orientations of 30° and 0° deformed only elastically and show brittle material behaviour. The toughness is the measure of material's ability to absorb energy before it breaks and it can be measured by the area under the stress strain curve. In term of identifying toughest specimens among all these five specimens, Figure 9 shows that the specimen printed with the orientations of 45° produced a specimen with high toughness, and for the specimen with the orientations of 90°, 30°, 60° and 0° produced specimens with gradually reduction of the value of toughness from high to low respectively.

b. Outer surface observations of tensile specimens

Figure 10 shows SEM micrographs of outer top surfaces of the tensile specimens. These micrographs confirmed the printed patterns formed with five different raster orientations.

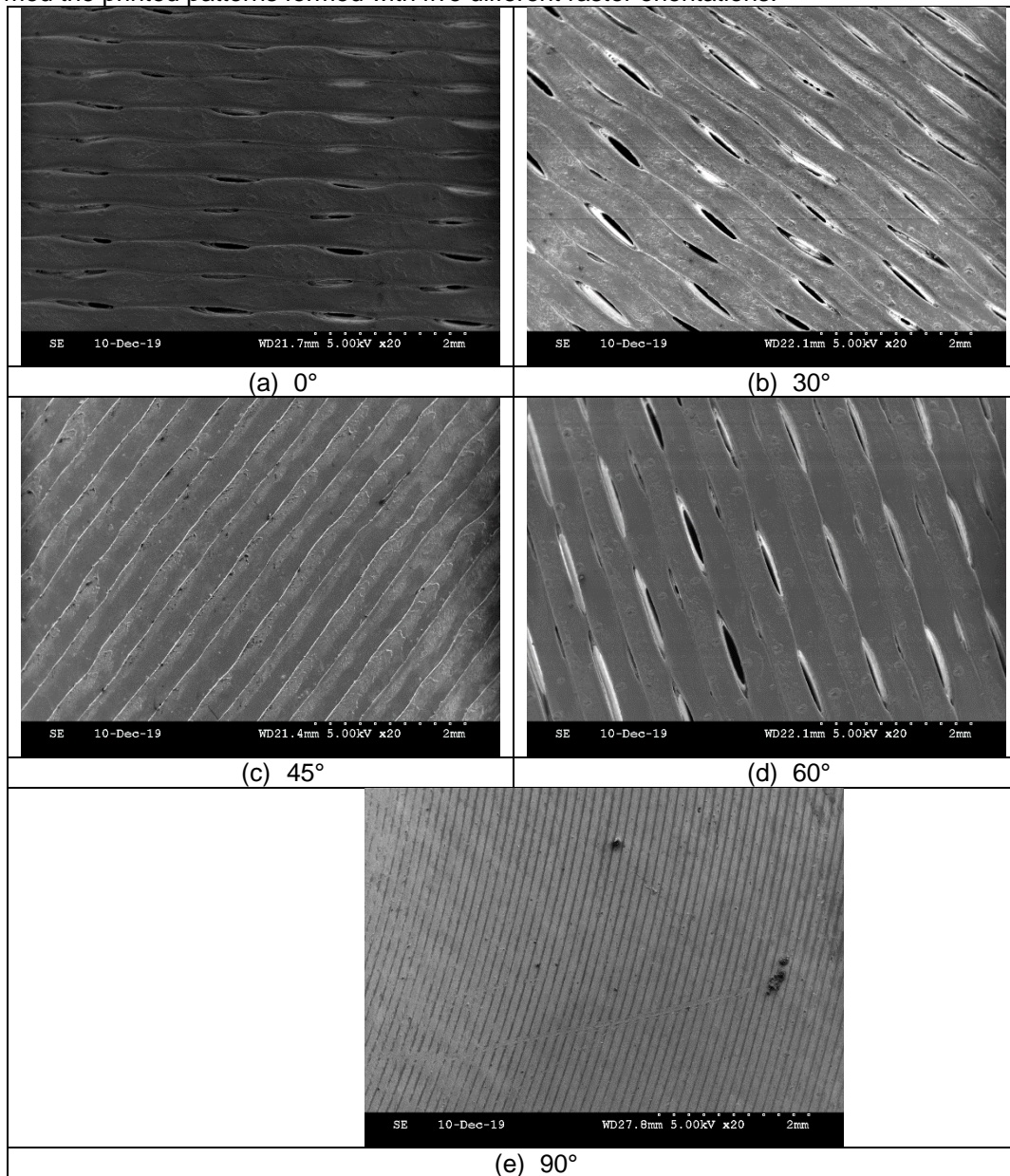


Figure 10: SEM micrographs represent printing patterns those are formed with five different raster orientations (a) 0°, (b) 30°, (c) 45°, (d) 60° and (e) 90°.

c. Fracture interface observations after tensile test

Figure 11 shows SEM micrographs of fracture interface of tensile specimens with five raster angles (a) 0°, (b) 30°, (c) 45°, (d) 60° and (e) 90°. As shown in Figure 11 (a, b and d) the specimens got ruptured along the layers and formed smooth fractured surfaces, which indicates that the raster angles 0°, 30° and 60° are not given the opportunity to the material to resist the tensile load instead of this the specimens failed due to poor interfacial adhesion between the layers. The specimens formed with these raster orientations are not effectively transferred tensile load from one layer to another layer so that small tensile strength and tensile modulus were attained. However, in the contrary, the specimens formed with the raster angles 45° and 90° are showed rough fractured surfaces as shown Figure 11 (c) and (e), and these specimens are featured due to material failing during tensile loading so that larger tensile strength and tensile modulus were achieved.

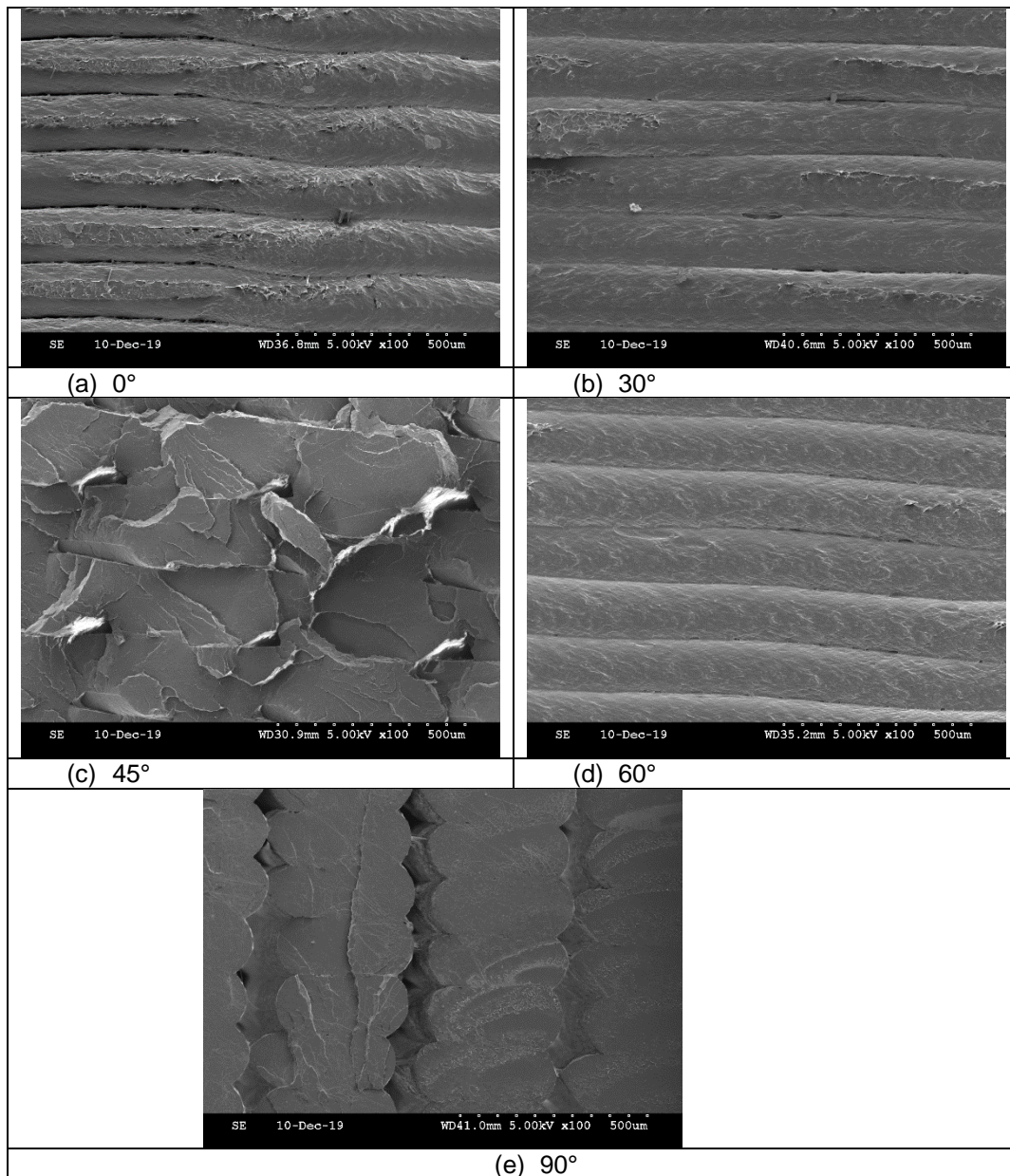


Figure 11: SEM images of fractured interface of tensile specimens with five raster angles a. 0°, b. 30°, c. 45°, d. 60° and e. 90°.

d. 3D printing defects

Any defects such as openings, cracks, voids and air gaps in 3D printed parts are adversely affected on part material properties. Therefore, these defects are needed to be avoided in the final finished form of the 3D printed part. In this study, SEM microstructure images are used to identify these defects in 3D printed specimens that were fabricated using five different raster orientations. Figure 13 shows SEM microstructure images for the outer top surfaces of the all five specimens and identified several problems with the print quality. These problems are most notable in the specimens that are printed with the 0°, 30° and 60° raster angles as shown in Figure 13 (a), (b) and (d). The outer surfaces of these specimens showed the cracks in between two rasters, these rasters are not properly bonded with each other during printing and caused inner layer cracks on outer face of the printed specimens. The averaged crack lengths for the specimens printed with 0°, 30° and 60° raster orientations are 0.7 mm, 0.8 mm and 1.2 mm respectively. It showed that the specimens printed with 60° raster angle formed larger cracks compared to the raster angles 0° and 30°. In 3D printing process, the rapid heating and cooling cycle of the material causes non-uniform thermal gradient and produces thermal stresses within the material. These stresses cause deformations in inner layer or form cracks in two adjacent

rasters, which cause dimensional inaccuracy and de-lamination. The specimen with 60° raster angle is more prone to deform by these stresses and cause large cracks and openings compared to other two raster angles. This might be because, it is more difficult to the material for the regain its original shape or dimension completely after the melting at the angle of 60°. In contrast of this, the specimens with raster angles with 45° and 90° formed compact outer surfaces and any defect cannot be seen on them as shown in Figure 13 (c) and (e). Also, the curve edge of the tensile specimen fabricated with 45° raster angle is examined by SEM and images are shown in Figure 12. It shows that 45° raster angle formed a good quality of 3D print and solve the problems near the radius section of the tensile specimen that were identified earlier in the specimen fabricated with the raster angle 0° [37].

In this study, the fracture interface of all five tensile specimens printed with five different raster orientation were investigated to explore internal quality of 3D printed specimens. Figure 14 shows the SEM images for all five fracture interfaces that formed after tensile test. These images identified several problems in the placement of layers of 3D printing process. The specimens fabricated with the raster orientations of 0°, 30° and 60° formed series of air gaps between the layers all along the thickness of the specimen that can be seen in Figure 14 (a), (b) and (d). In Figure 14 (e) shows the far edge of the fracture interface for the specimen formed with raster angle 60° and clearly identified the air gaps in the placement of layers and to adjacent rasters. Moreover, the Figure 14 (c) shows the fracture interface of the specimen printed with raster angle 45° and identified the triangular voids of average 2200 μm^2 between the two layers. Similarly, the Figure 14 (f) shows the fracture interface of the specimen printed with raster angle 90° and identified the diamond shape openings of average 18000 μm^2 between the two layers. These defects in 3D printed specimens can be caused due to temperature variations during the placement of layers. In FDM process, the 3D printer deposits the filaments layer by layer and these layers bond by local re-melting of previously solidified material. These openings, air gaps and voids can be formed because of the non-uniform heating and cooling during printing process. This non-uniformed temperature gradient causes non-uniformed stresses and produces deformations [34]. Overall, the specimens fabricated with the raster orientations of 0°, 30° and 60° identified printed defects in both outer and inner surfaces of the specimens. These defects directly affected on specimen's material strength and formed weaker specimens. In this study, the specimens fabricated with the raster orientations of 0°, 30° and 60° showed less tensile strength compared to the specimens fabricated with the raster orientations of 90° and 45°. Although, the specimens fabricated with the raster orientations of 90° and 45° formed good outer surfaces of the specimens and any defect cannot be seen on outer faces of these specimens. However, some inner defects can still be seen on the fracture interfaces for these specimens. It is clearly evident that the strength of these specimens can be further improved by avoiding these printing problems and defects. Thus, raster orientation is affected on 3D printed part strength, accuracy and surface finish. Suitable selection of this angle can increase the strength of the part by reducing the gaps between the deposited layers, by reducing these gaps, and better surface finish can be achieved specially for the difficult sections of a part such as curved surfaces.

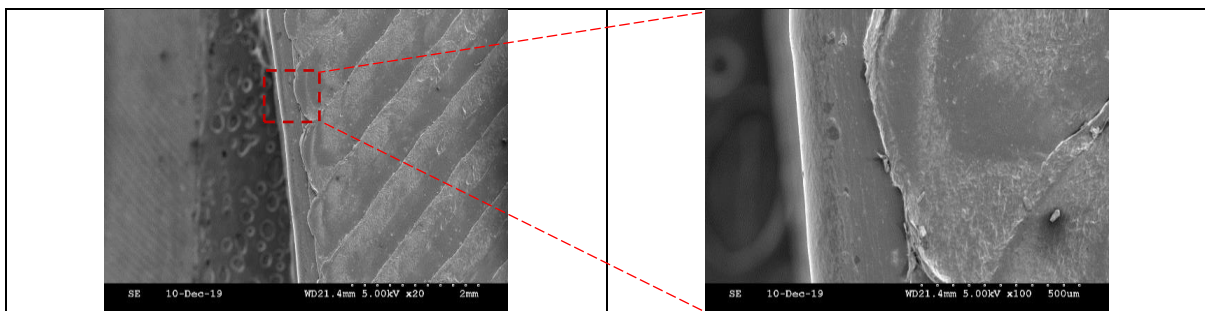


Figure 12: SEM images of the curve edge of the tensile specimen fabricated with 45° raster angle.

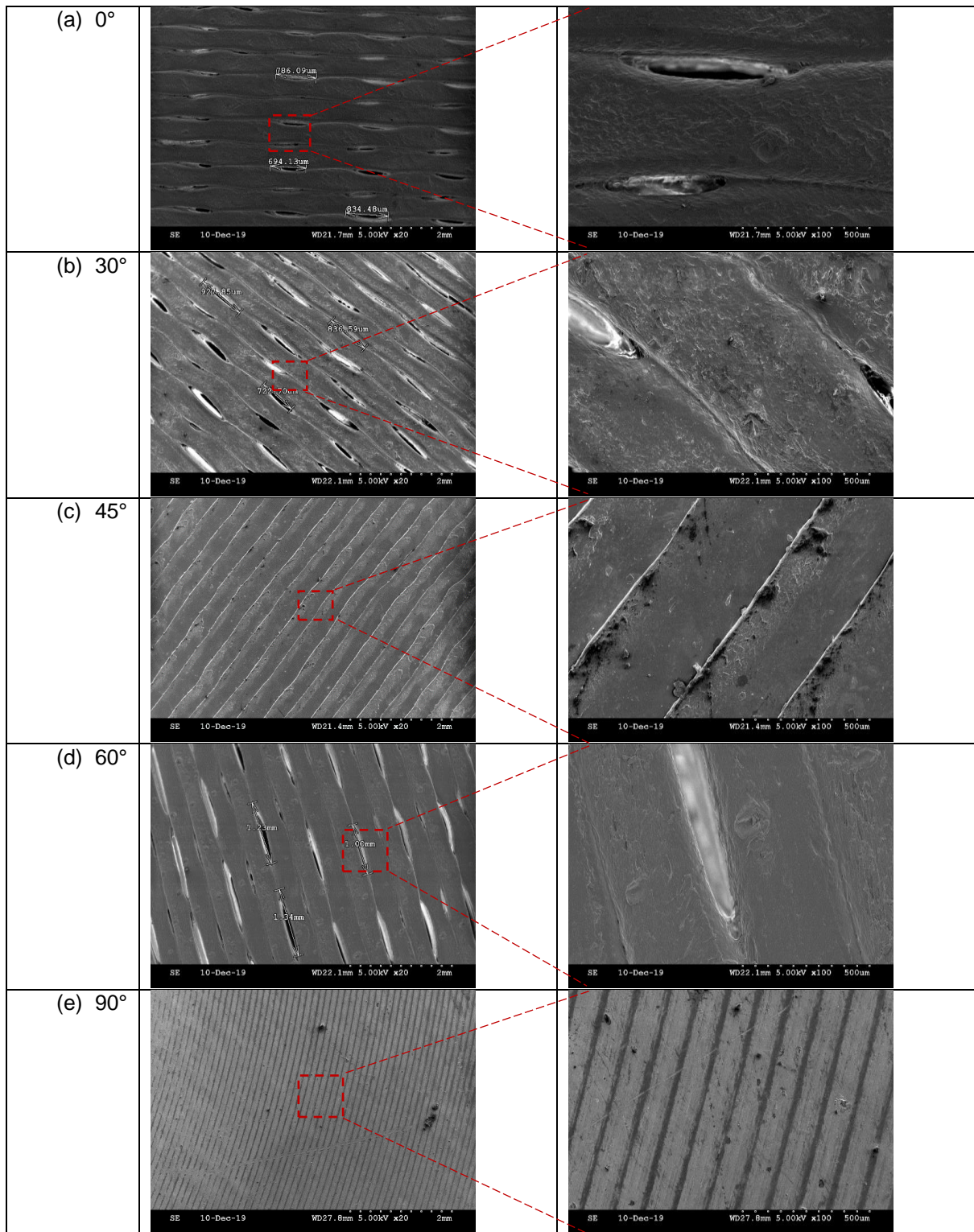
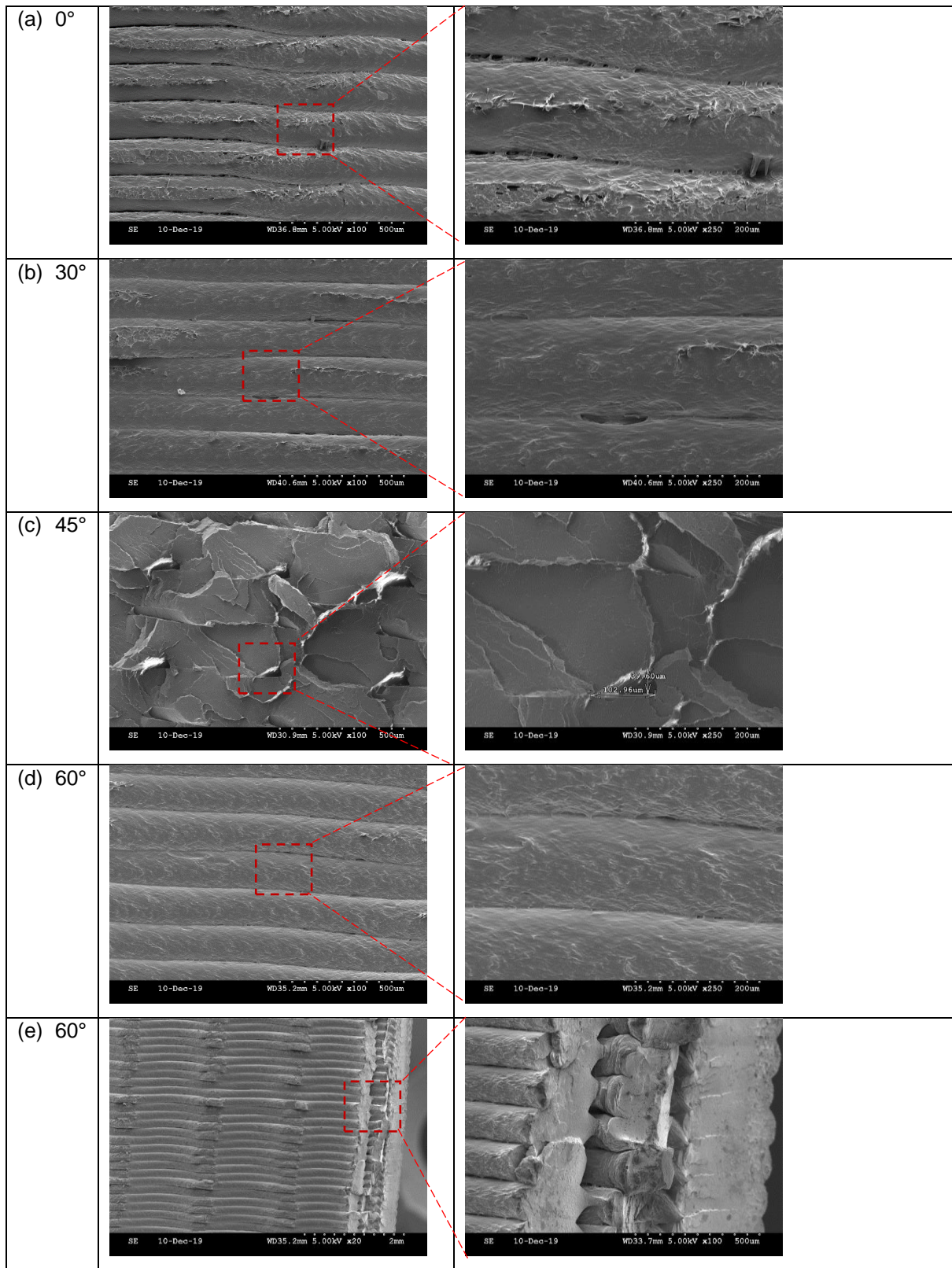


Figure 13: SEM images of outer surface of the specimens show the defects-openings or cracks for the orientation of 0°, 30°, 45°, 60° and 90°.



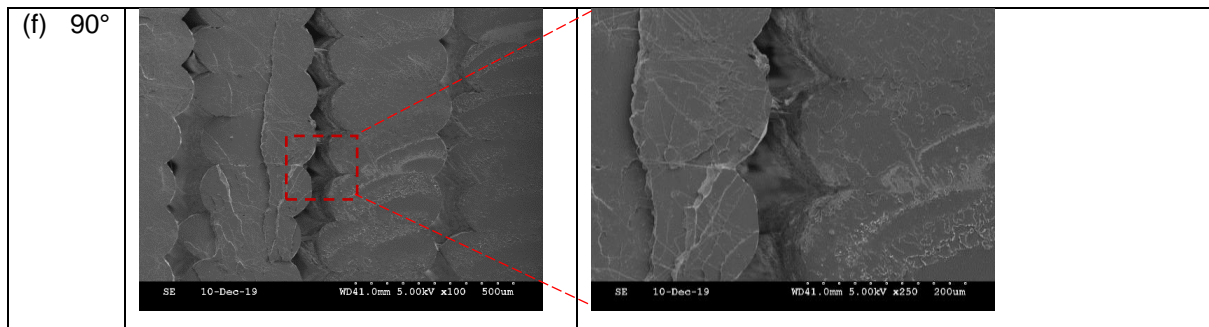


Figure 14: SEM images show the fracture interface formed after tensile test of the specimens fabricated with five different raster orientations.

Conclusion

In this study, the five different raster angles were used to fabricate the 3D printed specimens using PLA material. The tensile properties for all these specimens were investigated to identify the best raster position to fabricate the strongest 3D printed part. In this study, the fracture interface of these specimens after tensile testing were also examined using a scanning electron microscopy (SEM) to explain material failure modes and reasons. In this study, the micro-level structural changes on outer and inner surfaces of these 3D printed specimens due to use of different raster orientations were also assessed. The following conclusions are drawn from this study.

- The position of raster is an important parameter for 3D printing process, and it has a vital role in the specimen strength, accuracy and surface finish. The 45° raster orientation produced a strongest specimen with the average ultimate tensile is 55.45 MPa and highest elongation of 4.24 %. The 90° raster orientation produced the second highest strength compared to the results of all other printed specimens.
- The specimens fabricated with the raster angles 0°, 30° and 60° formed smooth fractured surfaces, which identify that the specimens with these orientations are not given the opportunity to the material to resist the tensile load instead of this the specimens failed due to poor interfacial adhesion between the layers which gave the less value of tensile strength and tensile module were achieved. However, the specimens fabricated with the raster angles 45° and 90° showed rough fractured surfaces and these specimens are fractured due to material failing during tensile loading which gave larger tensile strength and tensile modules.
- The microstructural analysis identified that the outer surfaces of the specimens that are printed with the 0°, 30° and 60° raster angles showed the cracks between two rasters. In contrast of this, the specimens with raster angles with 45° and 90° formed compact outer surfaces that provide a better surface finish.
- Also, the micro level observations of fracture interface (inner surfaces) of all five specimens showed the series of air gaps and voids between the layers all along the thickness of the specimens.
- The specimens fabricated with the raster orientations of 0°, 30° and 60° identified several printing defects in both outer and inner surfaces of the specimens. Although, the specimens fabricated with the raster orientations of 90° and 45° formed compact outer surfaces and any defects cannot be seen on them at micro level and they provide better surface finish. However, some inner defects can still be seen on the fracture interfaces for these specimens. These microstructural observations can be correlated with the tensile strength results. The strength and accuracy of 3D parts can be further improved by avoiding printing problems and defects.

Acknowledgements

This work is carried out at University of Sunderland, the author would like to thank the University of Sunderland to provide fund for purchasing the 3D printing material. I like to thank Mr Carl Gregg at The Industrial Centre Sunderland to fabricate the 3D printed specimens. I also would like to thank Ms Kayleigh Ironside to provide her support and assistance in undertaking this SEM work.

References

- [1] Y. L. Yap, C. Wang, S. L. Sing, V. Dikshit, W. Y. Yeong, and J. Wei, 'Material jetting additive manufacturing: An experimental study using designed metrological benchmarks', *Precision engineering*, vol. 50, pp. 275–285, 2017.
- [2] N. Gupta, C. Weber, and S. Newsome, 'Additive manufacturing: status and opportunities', *Science and Technology Policy Institute, Washington*, 2012.
- [3] T. D. Ngo, A. Kashani, G. Imbalzano, K. T. Nguyen, and D. Hui, 'Additive manufacturing (3D printing): A review of materials, methods, applications and challenges', *Composites Part B: Engineering*, vol. 143, pp. 172–196, 2018.
- [4] K. C. Nune, A. Kumar, R. D. K. Misra, S. J. Li, Y. L. Hao, and R. Yang, 'Functional response of osteoblasts in functionally gradient titanium alloy mesh arrays processed by 3D additive manufacturing', *Colloids and Surfaces B: Biointerfaces*, vol. 150, pp. 78–88, 2017.
- [5] K. C. Nune, R. D. K. Misra, S. J. Li, Y. L. Hao, and R. Yang, 'Osteoblast cellular activity on low elastic modulus Ti–24Nb–4Zr–8Sn alloy', *Dental Materials*, vol. 33, no. 2, pp. 152–165, 2017.
- [6] B. Utela, D. Storti, R. Anderson, and M. Ganter, 'A review of process development steps for new material systems in three dimensional printing (3DP)', *Journal of Manufacturing Processes*, vol. 10, no. 2, pp. 96–104, 2008.
- [7] J. Kietzmann, L. Pitt, and P. Berthon, 'Disruptions, decisions, and destinations: Enter the age of 3-D printing and additive manufacturing', *Business Horizons*, vol. 58, no. 2, pp. 209–215, 2015.
- [8] H. Lipson and M. Kurman, *Fabricated: The new world of 3D printing*. John Wiley & Sons, 2013.
- [9] K. C. Nune, R. D. K. Misra, S. M. Gaytan, and L. E. Murr, 'Biological response of next-generation of 3D Ti-6Al-4V biomedical devices using additive manufacturing of cellular and functional mesh structures', *J Biomater Tissue Eng*, vol. 4, no. 10, pp. 755–771, 2014.
- [10] K. C. Nune, R. D. K. Misra, S. J. Li, Y. L. Hao, and R. Yang, 'Cellular response of osteoblasts to low modulus Ti-24Nb-4Zr-8Sn alloy mesh structure', *Journal of Biomedical Materials Research Part A*, vol. 105, no. 3, pp. 859–870, 2017.
- [11] T. Boland, T. Xu, B. Damon, and X. Cui, 'Application of inkjet printing to tissue engineering', *Biotechnology Journal: Healthcare Nutrition Technology*, vol. 1, no. 9, pp. 910–917, 2006.
- [12] X. Li *et al.*, '3D-printed biopolymers for tissue engineering application', *International Journal of Polymer Science*, vol. 2014, 2014.
- [13] S. Yang, K.-F. Leong, Z. Du, and C.-K. Chua, 'The design of scaffolds for use in tissue engineering. Part II. Rapid prototyping techniques', *Tissue engineering*, vol. 8, no. 1, pp. 1–11, 2002.
- [14] A. Kumar, K. C. Nune, L. E. Murr, and R. D. K. Misra, 'Biocompatibility and mechanical behaviour of three-dimensional scaffolds for biomedical devices: process–structure–property paradigm', *International Materials Reviews*, vol. 61, no. 1, pp. 20–45, 2016.
- [15] A. Kumar, K. C. Nune, and R. D. K. Misra, 'Biological functionality and mechanistic contribution of extracellular matrix-ornamented three dimensional Ti-6Al-4V mesh scaffolds', *Journal of Biomedical Materials Research Part A*, vol. 104, no. 11, pp. 2751–2763, 2016.
- [16] A. Kumar, K. C. Nune, and R. D. K. Misra, 'Biological functionality of extracellular matrix-ornamented three-dimensional printed hydroxyapatite scaffolds', *Journal of Biomedical Materials Research Part A*, vol. 104, no. 6, pp. 1343–1351, 2016.
- [17] Q. Shi *et al.*, 'Recyclable 3D printing of vitrimer epoxy', *Materials Horizons*, vol. 4, no. 4, pp. 598–607, 2017.
- [18] X. Tian, T. Liu, Q. Wang, A. Dilmurat, D. Li, and G. Ziegmann, 'Recycling and remanufacturing of 3D printed continuous carbon fiber reinforced PLA composites', *Journal of cleaner production*, vol. 142, pp. 1609–1618, 2017.
- [19] B. P. Conner *et al.*, 'Making sense of 3-D printing: Creating a map of additive manufacturing products and services', *Additive Manufacturing*, vol. 1, pp. 64–76, 2014.
- [20] C. C. Kai, L. K. Fai, and L. Chu-Sing, *Rapid prototyping: principles and applications in manufacturing*. Singapore: World Scientific Publishing Co., Inc., 2003.
- [21] S. Zhao *et al.*, 'Compressive and fatigue behavior of functionally graded Ti-6Al-4V meshes fabricated by electron beam melting', *Acta Materialia*, vol. 150, pp. 1–15, 2018.
- [22] L.-C. Zhang, H. Attar, M. Calin, and J. Eckert, 'Review on manufacture by selective laser melting and properties of titanium based materials for biomedical applications', *Materials Technology*, vol. 31, no. 2, pp. 66–76, 2016.
- [23] L. Novakova-Marcincinova, J. Novak-Marcincin, J. Barna, and J. Torok, 'Special materials used in FDM rapid prototyping technology application', in *2012 IEEE 16th International Conference on Intelligent Engineering Systems (INES)*, Lisbon, Portugal, 2012, pp. 73–76.

- [24] P. Dudek, 'FDM 3D printing technology in manufacturing composite elements', *Archives of Metallurgy and Materials*, vol. 58, no. 4, pp. 1415–1418, 2013.
- [25] A. Lanzotti, M. Grasso, G. Staiano, and M. Martorelli, 'The impact of process parameters on mechanical properties of parts fabricated in PLA with an open-source 3-D printer', *Rapid Prototyping Journal*, vol. 21, no. 5, pp. 604–617, 2015.
- [26] B. Wittbrodt and J. M. Pearce, 'The effects of PLA color on material properties of 3-D printed components', *Additive Manufacturing*, vol. 8, pp. 110–116, Oct. 2015, doi: 10.1016/j.addma.2015.09.006.
- [27] M. N. Hafsa, M. Ibrahim, M. Wahab, and M. S. Zahid, 'Evaluation of FDM pattern with ABS and PLA material', in *Applied Mechanics and Materials*, 2014, vol. 465, pp. 55–59.
- [28] J. Jiang, L. Su, K. Zhang, and G. Wu, 'Rubber-toughened PLA blends with low thermal expansion', *Journal of Applied Polymer Science*, vol. 128, no. 6, pp. 3993–4000, 2013.
- [29] J. Hughes, R. Thomas, Y. Byun, and S. Whiteside, 'Improved flexibility of thermally stable polylactic acid (PLA)', *Carbohydrate polymers*, vol. 88, no. 1, pp. 165–172, 2012.
- [30] J. Comb, W. Priedeman, and P. W. Turley, 'FDM® Technology process improvements', in *1994 International Solid Freeform Fabrication Symposium*, Austin, United States, 1994.
- [31] R. H. Sanatgar, C. Campagne, and V. Nierstrasz, 'Investigation of the adhesion properties of direct 3D printing of polymers and nanocomposites on textiles: Effect of FDM printing process parameters', *Applied Surface Science*, vol. 403, pp. 551–563, 2017.
- [32] O. A. Mohamed, S. H. Masood, and J. L. Bhowmik, 'Optimization of fused deposition modeling process parameters: a review of current research and future prospects', *Advances in Manufacturing*, vol. 3, no. 1, pp. 42–53, 2015.
- [33] K. Chin Ang, K. Fai Leong, C. Kai Chua, and M. Chandrasekaran, 'Investigation of the mechanical properties and porosity relationships in fused deposition modelling-fabricated porous structures', *Rapid Prototyping Journal*, vol. 12, no. 2, pp. 100–105, 2006.
- [34] A. K. Sood, R. K. Ohdar, and S. S. Mahapatra, 'Parametric appraisal of mechanical property of fused deposition modelling processed parts', *Materials & Design*, vol. 31, no. 1, pp. 287–295, 2010.
- [35] A. W. Fatimatuzahraa, B. Farahaina, and W. A. Y. Yusoff, 'The effect of employing different raster orientations on the mechanical properties and microstructure of Fused Deposition Modeling parts', in *2011 IEEE Symposium on Business, Engineering and Industrial Applications (ISBEIA)*, Langkawi, Malaysia, 2011, pp. 22–27.
- [36] A. Rodríguez-Panes, J. Claver, and A. M. Camacho, 'The Influence of Manufacturing Parameters on the Mechanical Behaviour of PLA and ABS Pieces Manufactured by FDM: A Comparative Analysis', *Materials*, vol. 11, no. 8, p. 1333, Aug. 2018, doi: 10.3390/ma11081333.
- [37] T. Letcher and M. Waytashek, 'Material property testing of 3D-printed specimen in PLA on an entry-level 3D printer', in *ASME 2014 international mechanical engineering congress and exposition*, Montreal, Canada, 2014, p. V02AT02A014–V02AT02A014.
- [38] 'GoPrint3D - 3D Printer Specialists'. <https://www.goprint3d.co.uk> (accessed Dec. 17, 2019).
- [39] D20 Committee, 'Test Method for Tensile Properties of Plastics', ASTM International. doi: 10.1520/D0638-10.